SAND2021-6131C

Sandia National Laboratories

Exceptional service in the national interest

Topology Optimization for Ductile Failure and Buckling Resistance

World Congress on Structural and Multidisciplinary Optimization – June 2021

Jonathan B. Russ

Research performed partially at Columbia University & Sandia National Laboratories

Sandia National Laboratories is a multimission laboratory managed and operated by National Technology and Engineering Solutions of Sandia LLC, a wholly owned subsidiary of Honeywell International Inc. for the U.S. Department of Energy's National Nuclear Security Administration under contract DE-NA0003525.

Outline

- Motivation
- Numerical models used during optimization
- Optimization problem formulation
- Constitutive model calibration
- Numerical examples
- Slight modification to original optimization problem
- Concluding remarks

Motivation

- **Goal:** Increasing the *peak load capacity* of a structure, in addition to the *structural toughness*
- **Proposal:** an elastoplastic topology optimization formulation which incorporates *both* ductile failure and buckling resistance

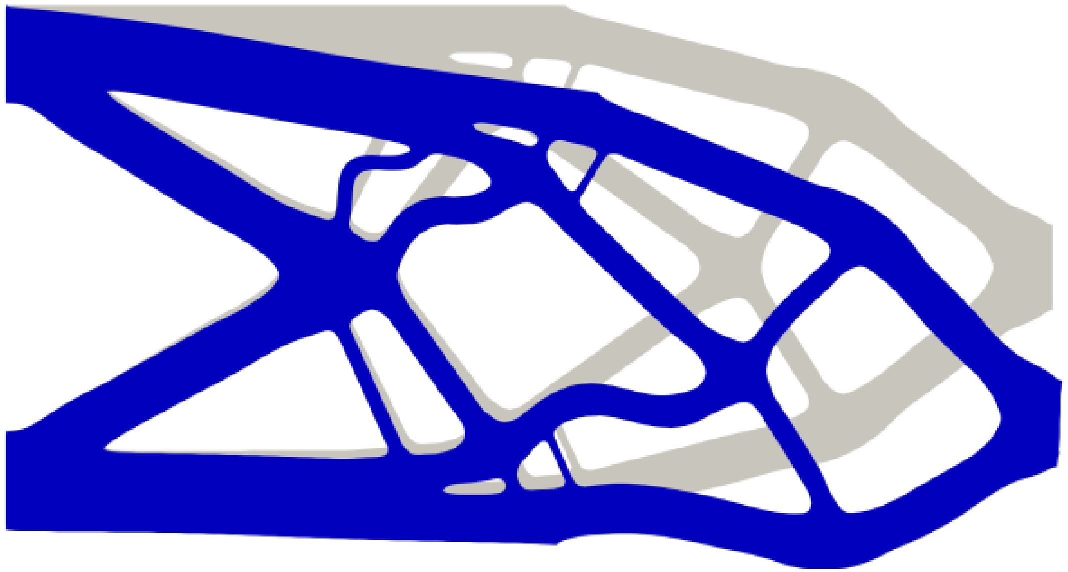

Maximize Total Work Only

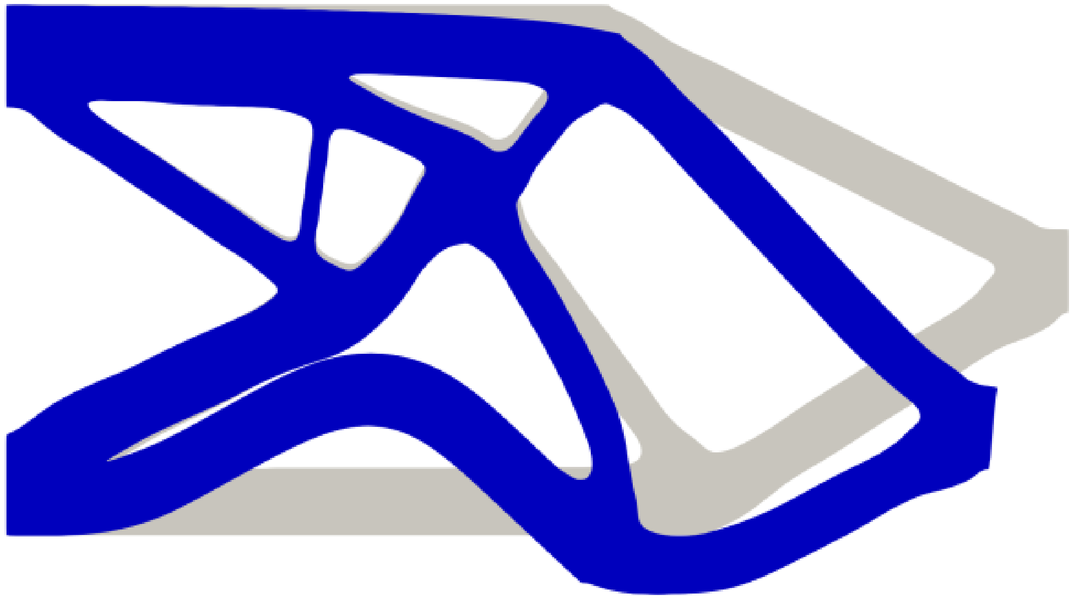

Maximize Total Work With Ductile Failure Constraints

Macroscopic view of proposed procedure

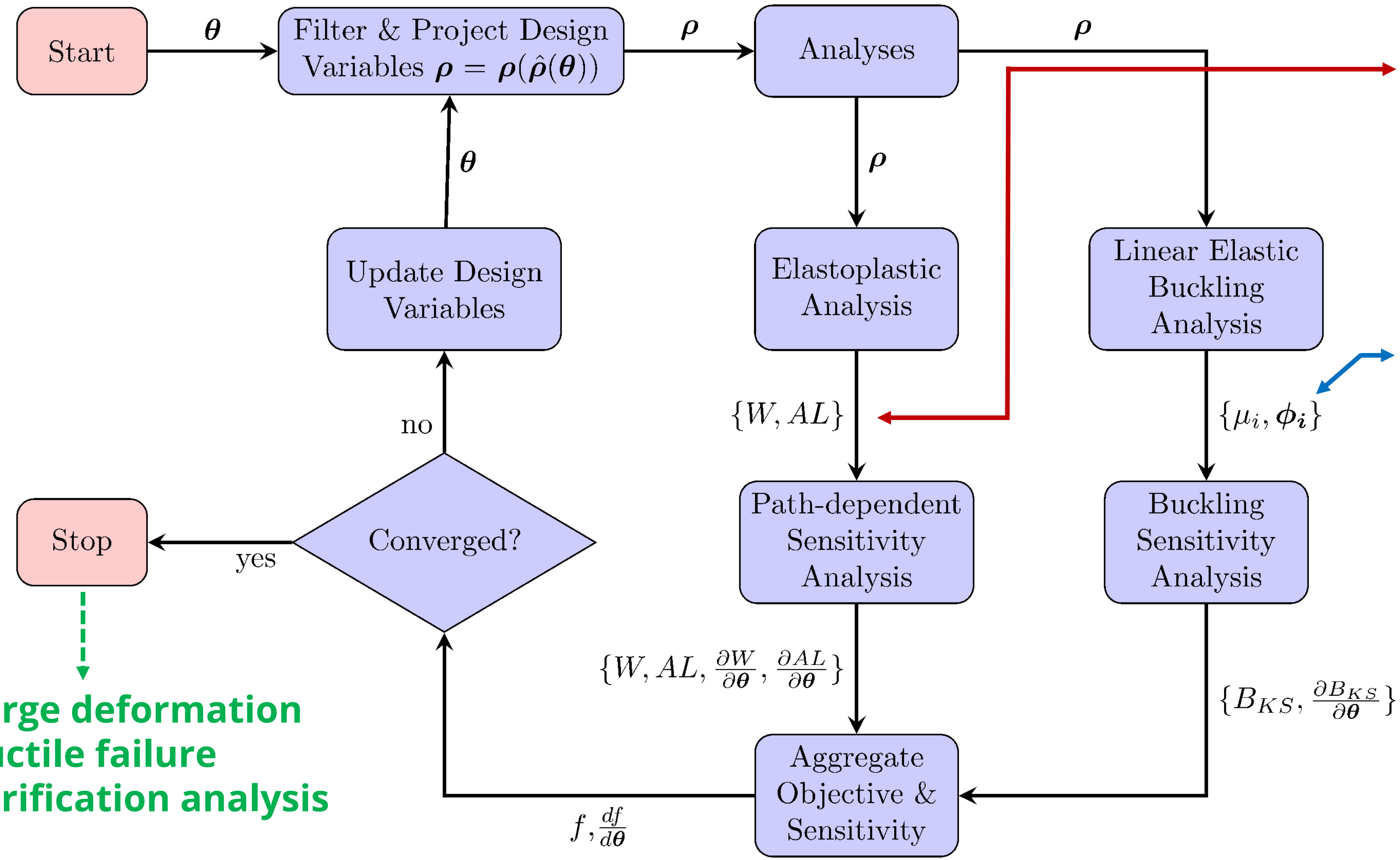

Elastoplastic Analysis
Compute:
(1) total work
(2) local ductile failure indicators

Linear Elastic Buckling Analysis
Compute:
(1) buckling load factors
(2) buckling mode shapes

Large deformation ductile failure verification analysis

Elastoplastic model used during optimization procedure

- Small-strain J_2-plasticity model with nonlinear hardening law

Global Residual Equations:

$$\boldsymbol{R}^e_{n+1} = \int_{\Omega_e} \boldsymbol{B}^{u^T} : \boldsymbol{s}_{n+1}\, dV + \left(\frac{\kappa}{V_e} \int_{\Omega_e} \boldsymbol{B}^u_{div} \bar{\boldsymbol{u}}_{n+1}\, dV \right) \left(\int_{\Omega_e} \boldsymbol{B}^{u^T}_{div}\, dV \right)$$

Local Residual Equations:

If Elastic Step:

$$\boldsymbol{H}^{e_q}_n = \begin{bmatrix} \alpha_n - \alpha_{n-1} \\ \Delta\gamma_n \\ \boldsymbol{\varepsilon}^p_n - \boldsymbol{\varepsilon}^p_{n-1} \end{bmatrix} = \begin{bmatrix} 0 \\ 0 \\ \mathbf{0} \end{bmatrix}$$

If Plastic Step:

$$\boldsymbol{H}^{e_q}_n = \begin{bmatrix} \alpha_n - \alpha_{n-1} - \Delta\gamma_n \\ \sqrt{\frac{3}{2} \boldsymbol{s}_n : \boldsymbol{s}_n} - \sigma_y(\alpha_n) \\ \boldsymbol{\varepsilon}^p_n - \boldsymbol{\varepsilon}^p_{n-1} - \Delta\gamma_n \boldsymbol{N}_n \end{bmatrix} = \begin{bmatrix} 0 \\ 0 \\ \mathbf{0} \end{bmatrix}$$

Voce-type hardening law: $\sigma_y(\alpha) = \sigma_{y_0} + H\alpha + Y_\infty \left(1 - \exp\left(-\delta\alpha\right)\right)$

Buckling analysis used during optimization procedure

- Small-strain linear elasticity $$\boldsymbol{K}_L \bar{\boldsymbol{u}}_L = \boldsymbol{f}_0$$

Buckling load factors

- Linear elastic buckling eigenproblem $$\boldsymbol{K}_\sigma \boldsymbol{\phi}_i = \mu_i \boldsymbol{K}_L \boldsymbol{\phi}_i \quad \text{where } \lambda_i = -1/\mu_i$$
- Transformed eigenproblem $$\left(\boldsymbol{K}_L + \boldsymbol{K}_\sigma\right) \boldsymbol{\phi}_i = \bar{\mu}_i \boldsymbol{K}_L \boldsymbol{\phi}_i \quad \text{where } \mu_i = 1.0 - \bar{\mu}_i$$
- Buckling aggregation function $$B_{KS} = \frac{1}{\xi_{ks}} \ln \left(\sum_{i \in \mathcal{B}} \exp\left(\xi_{ks} \mu_i\right) \right)$$

Employed buckling formulation largely consistent with:
Ferrari, F., Sigmund, O., 2019. Revisiting topology optimization with buckling constraints. Struct Multidisc Optim 59, 1401–1415.

SIMP Density Filter / Projection Operations

- Helmholtz PDE filter used to mitigate typical mesh instabilities

$$-r^2\nabla^2\hat{\rho} + \hat{\rho} = \theta \text{ , in the domain, } \Omega$$
$$\nabla\hat{\rho}\cdot\boldsymbol{n} = 0 \text{ , on the boundary, } \partial\Omega$$

θ Design Variables
$\hat{\rho}$ Filtered Design Variables
ρ Projected & Filtered Variables

- Smooth Heaviside hyperbolic tangent projection used to obtain 0/1 designs with continuation on the projection parameter

$$\rho_e(\hat{\rho}_e(\boldsymbol{\theta})) = \frac{\tanh(\beta\eta) + \tanh(\beta(\hat{\rho}_e - \eta))}{\tanh(\beta\eta) + \tanh(\beta(1-\eta))}$$

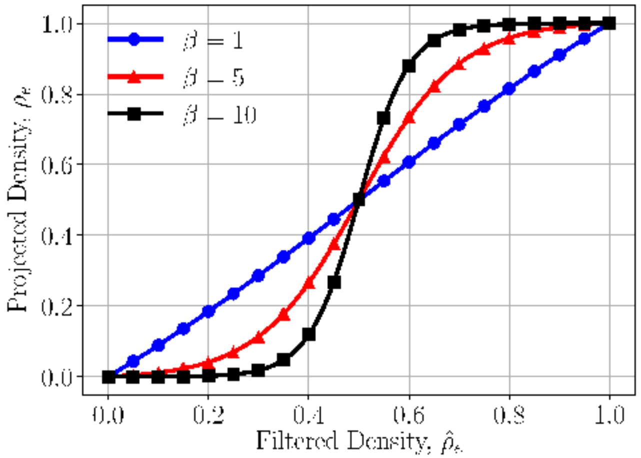

Lazarov, B.S., Sigmund, O., 2011. Filters in topology optimization based on Helmholtz-type differential equations. IJNME.
Guest et al., 2004. Achieving minimum length scale in topology optimization using nodal design variables and projection functions. IJNME.

Optimization problem formulation

Elastoplastic Analysis

Linear Elastic Buckling Analysis

Maximize Total Work | Maximize Buckling Load Factors | Enforce Local Ductile Failure Constraints

$$\underset{\boldsymbol{\theta}}{\text{minimize}} \quad -\omega_1 \frac{W(\boldsymbol{\theta}, \{\bar{\boldsymbol{u}}_i\}, \{\boldsymbol{c}_i\})}{W^{scale}} + \omega_2 \frac{B_{KS}(\boldsymbol{\theta}, \bar{\boldsymbol{u}}_L)}{B_{KS}^{scale}} + \omega_3 \; AL(\boldsymbol{\theta}, \{\bar{\boldsymbol{u}}_i\}, \{\boldsymbol{c}_i\})$$

$$\text{subject to} \quad 0 \leq \theta_e \leq 1, \; e = 1, \ldots, N_{elem}$$

Constrain Mass →

$$\Lambda(\boldsymbol{\theta}) \leq \Lambda_{max}$$

Elastoplastic Analysis Constraints →

$$\boldsymbol{R}^{(i)}(\boldsymbol{\theta}, \{\bar{\boldsymbol{u}}_i\}, \{\boldsymbol{c}_i\}) = \boldsymbol{0}, \; i = 1, \ldots, N_{steps}$$

$$\boldsymbol{H}^{(i)}(\boldsymbol{\theta}, \{\bar{\boldsymbol{u}}_i\}, \{\boldsymbol{c}_i\}) = \boldsymbol{0}, \; i = 1, \ldots, N_{steps}$$

Linear Elastic Buckling Analysis Constraints →

$$\boldsymbol{K}_L(\boldsymbol{\theta})\bar{\boldsymbol{u}}_L = \boldsymbol{f}_0$$

$$\boldsymbol{K}_\sigma(\boldsymbol{\theta}, \bar{\boldsymbol{u}}_L)\phi_i = \mu_i \boldsymbol{K}_L(\boldsymbol{\theta})\phi_i \text{ for } i \in \mathcal{B}$$

Augmented Lagrangian technique used to enforce local constraints at each quadrature point

$$D_{f_q} = \int_0^{\alpha_q^{final}} \frac{1}{\hat{d}_1 + \hat{d}_2 \exp\left(\hat{d}_3 \eta_q\right)} d\alpha_q \leq D_{max} \leq 1$$

Local ductile failure constraint enforcement

Local constraint: $D_{f_q} = \int_0^{\alpha_q^{final}} \frac{1}{\hat{d}_1 + \hat{d}_2 \exp\left(\hat{d}_3 \eta_q\right)} d\alpha_q \leq D_{max} \leq 1$

$$AL(\boldsymbol{\theta}, \{\bar{\boldsymbol{u}}_i\}, \{\boldsymbol{c}_i\}) = \sum_{q=1}^{N_{quad}} \left(\lambda_q g_q(\rho_e, D_{f_q}) + \frac{\mu_q}{2} g_q(\rho_e, D_{f_q})^2 \right)$$

Previously proposed constraint function form:

$$g_q(\rho_e, D_{f_q}) = \begin{cases} \rho_e^{0.5} \left(\frac{D_{f_q}}{D_{max}} - 1 \right)^2, & \text{if } D_{f_q} > D_{max} \\ 0, & \text{otherwise} \end{cases}$$

Modification to control nonlinearity and prevent entirely zero gradient:

$$g_q(\rho_e, D_{f_q}) = \begin{cases} \rho_e^{0.5} \left(\zeta_1 \left(\frac{D_{f_q}}{D_{max}} \right)^2 + (\zeta_2 - 2\zeta_1) \frac{D_{f_q}}{D_{max}} + \zeta_1 \right), & \text{if } D_{f_q} > D_{max} \\ \rho_e^{0.5} \zeta_2 \left(\frac{D_{f_q}}{D_{max}} \right), & \text{otherwise} \end{cases}$$

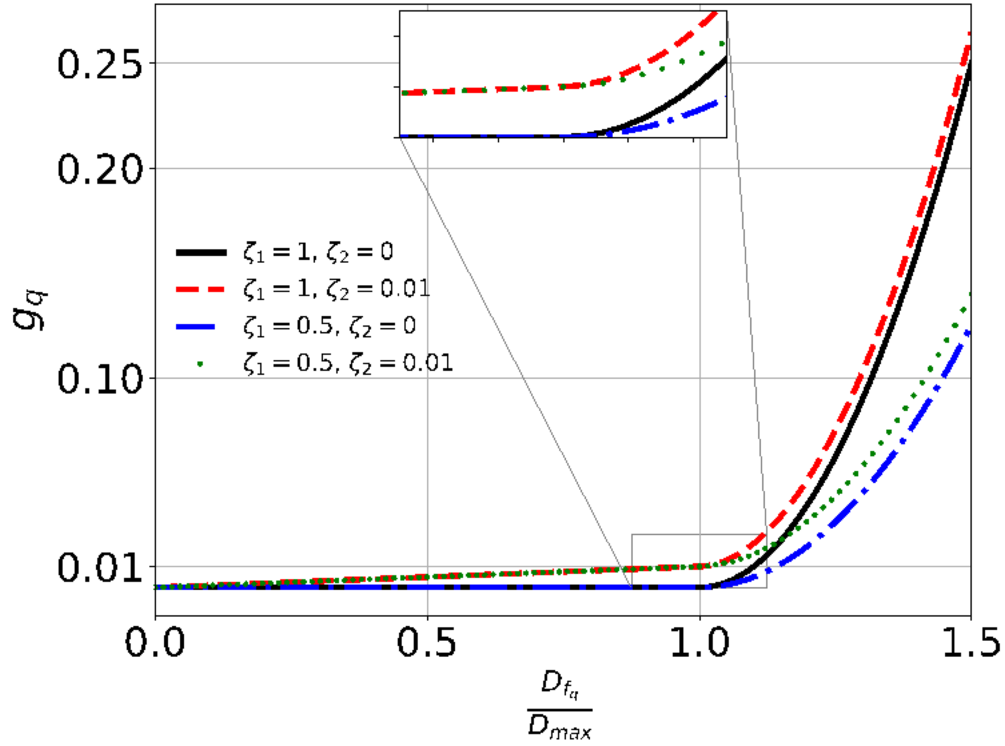

Senhora, F.V., Giraldo-Londoño, O., Menezes, I.F.M., Paulino, G.H., 2020. Topology optimization with local stress constraints: a stress aggregation-free approach. Struct Multidisc Optim.

Material model calibration (Aluminum 2024-T351)

Calibrated large deformation, ductile phase field fracture model to ***three*** round bar uniaxial tension experiments

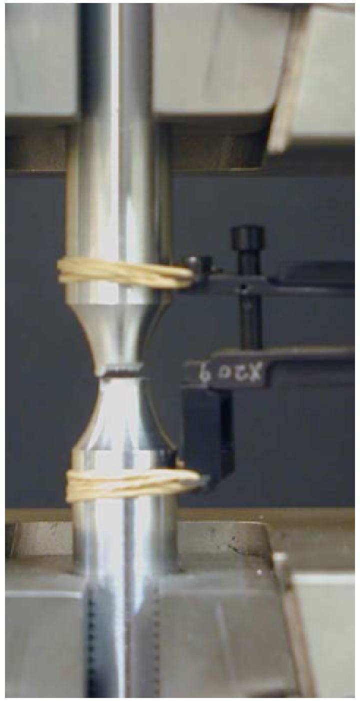

12mm Radius Notch Test

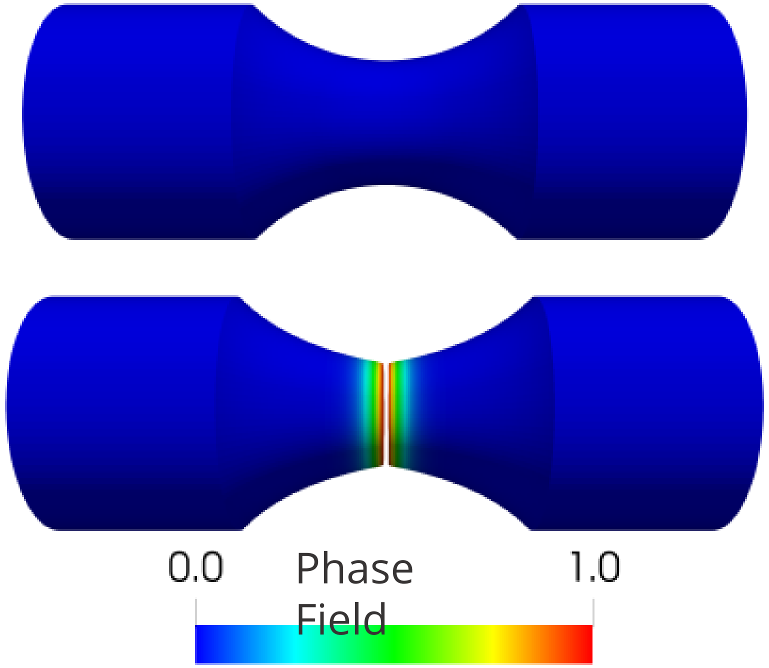

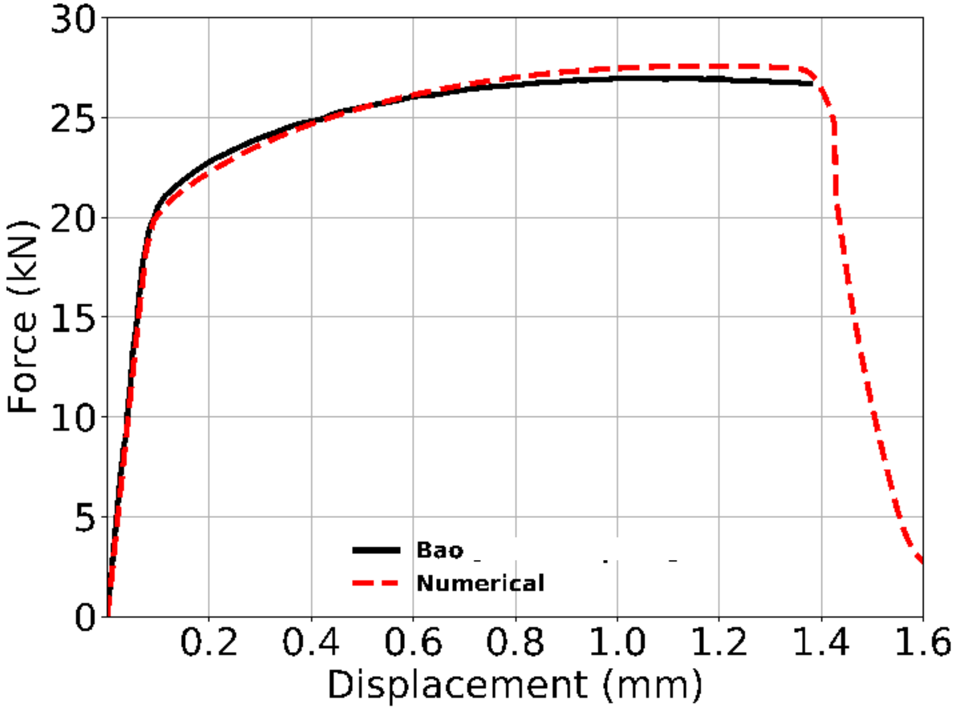

Bao, Y., Wierzbicki, T., 2004. On fracture locus in the equivalent strain and stress triaxiality space. International Journal of Mechanical Sciences 46, 81–98.
Borden et al. 2016. A phase-field formulation for fracture in ductile materials: Finite deformation balance law derivation, plastic degradation, and

Ductile failure criterion calibration (Aluminum 2024-T351)

Calibrated Johnson-Cook ductile failure criterion to the same ***three*** round bar uniaxial tension experiments

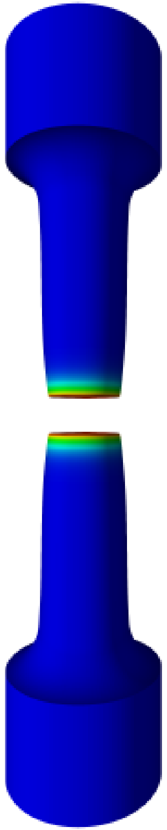

Smooth Bar

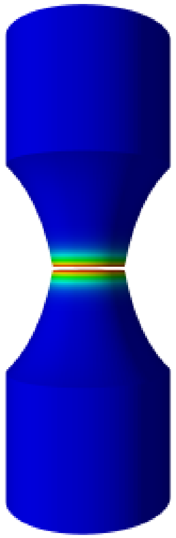

12mm Radius Notch

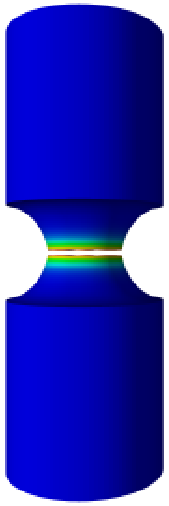

4mm Radius Notch

$$D_{f_q} = \int_0^{\alpha_q^{final}} \frac{1}{\hat{d}_1 + \hat{d}_2 \exp\left(\hat{d}_3 \eta_q\right)} d\alpha_q$$

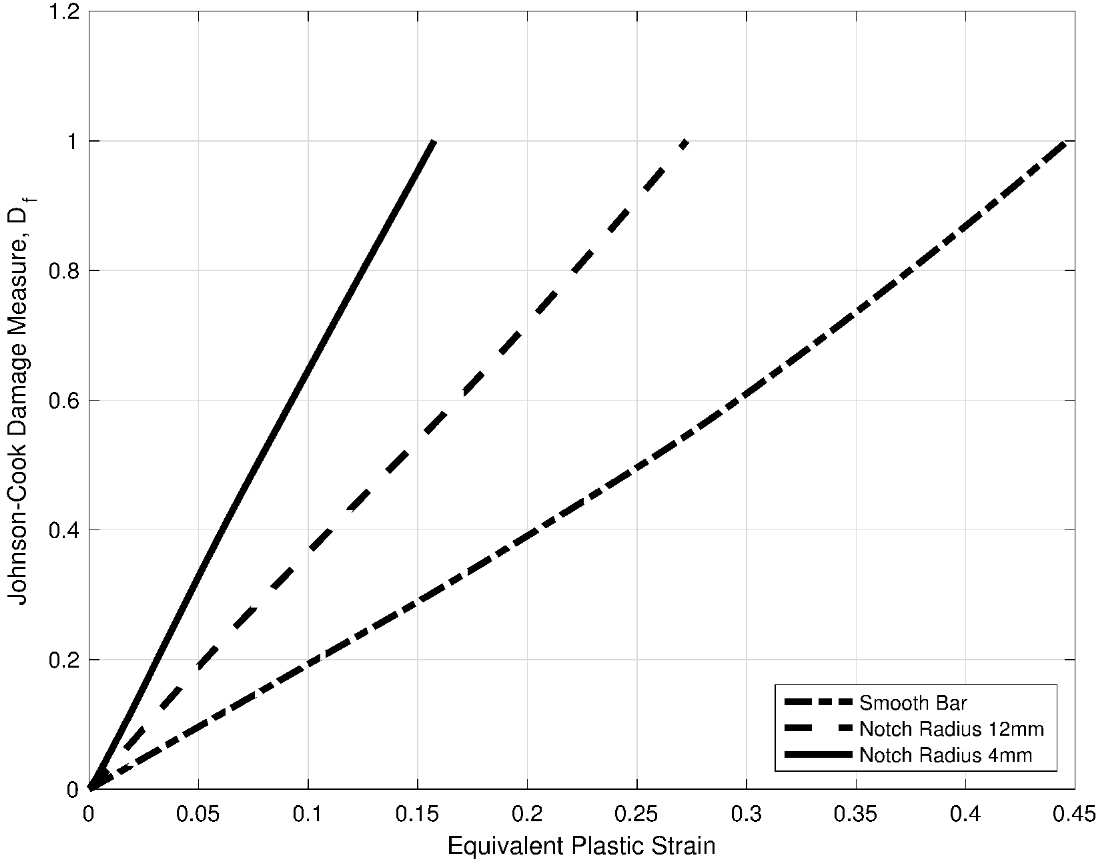

Bao, Y., Wierzbicki, T., 2004. On fracture locus in the equivalent strain and stress triaxiality space. International Journal of Mechanical Sciences 46, 81–98.

Alberdi, R.A., 2019. Computational Methods for Multiscale Analysis and Design of Nonlinear Multifunctional Materials and Structures for Energy

Cantilever beam numerical example

W: Design only maximizing total

WF: Design with ductile failure (omitting

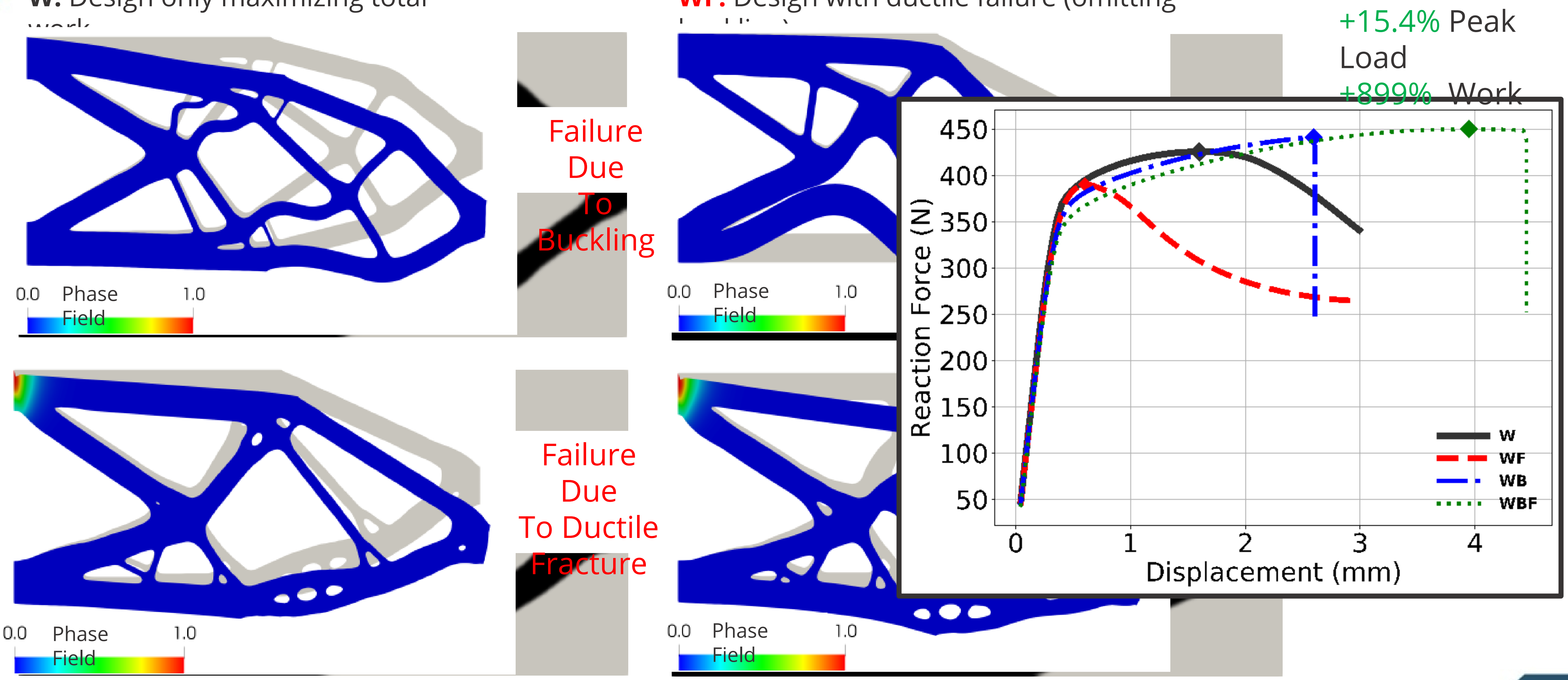

WB: Design with buckling only (omitting ductile

WBF: Design with ductile failure constraints and

Portal frame numerical example

W: Design only maximizing total work

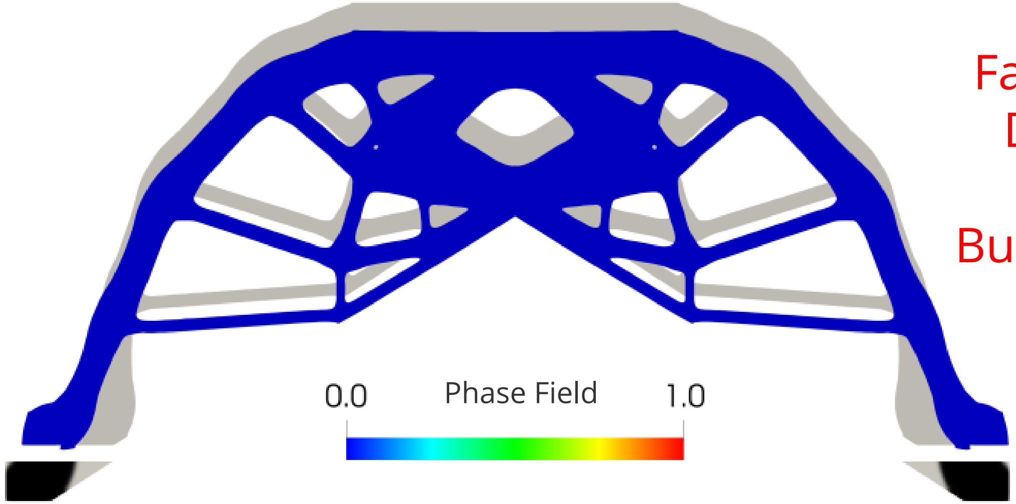

WF: Design with ductile failure (omitting buckling)

+5.2% Peak Load
+270% Work

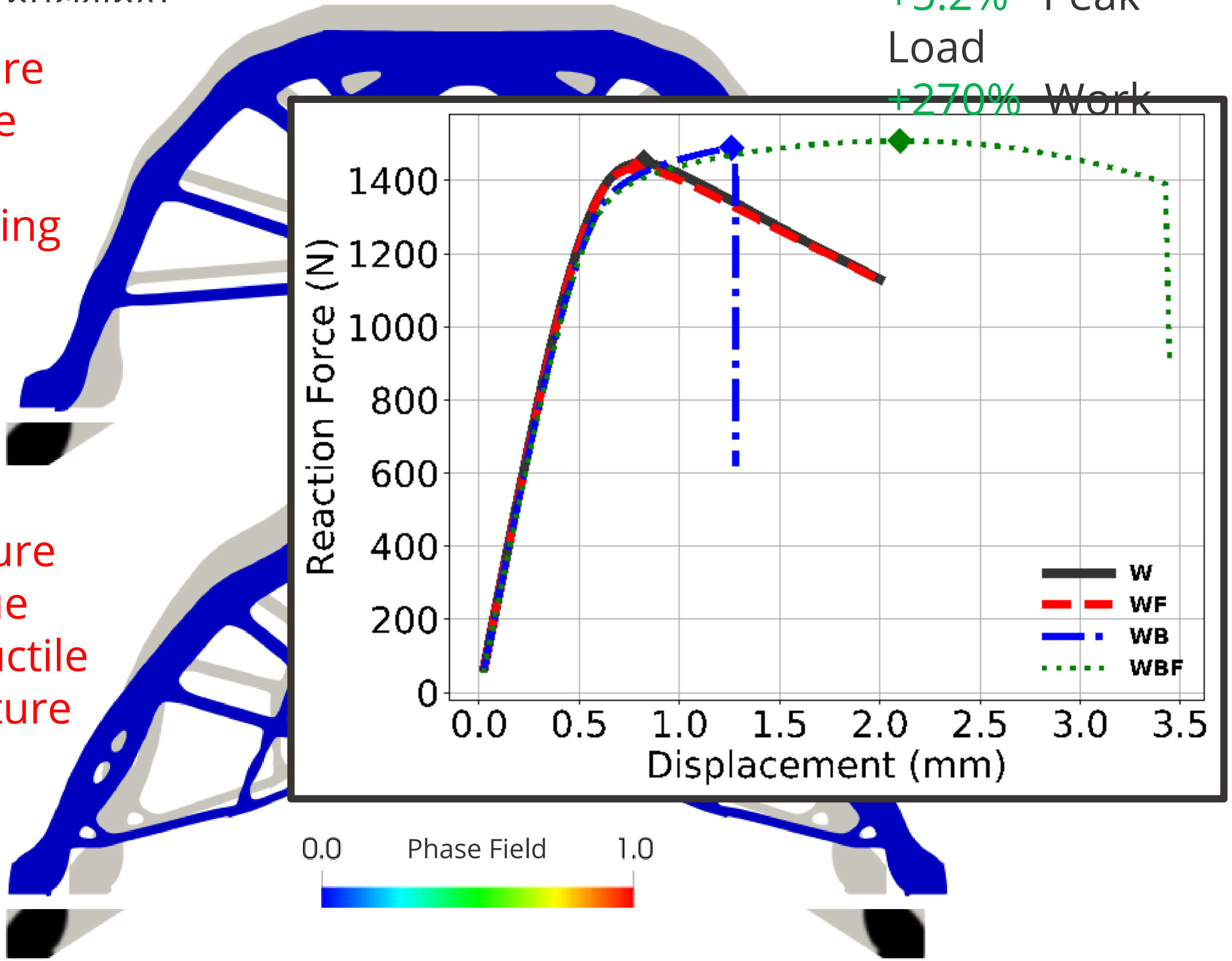

Failure Due To Buckling

Failure Due To Ductile Fracture

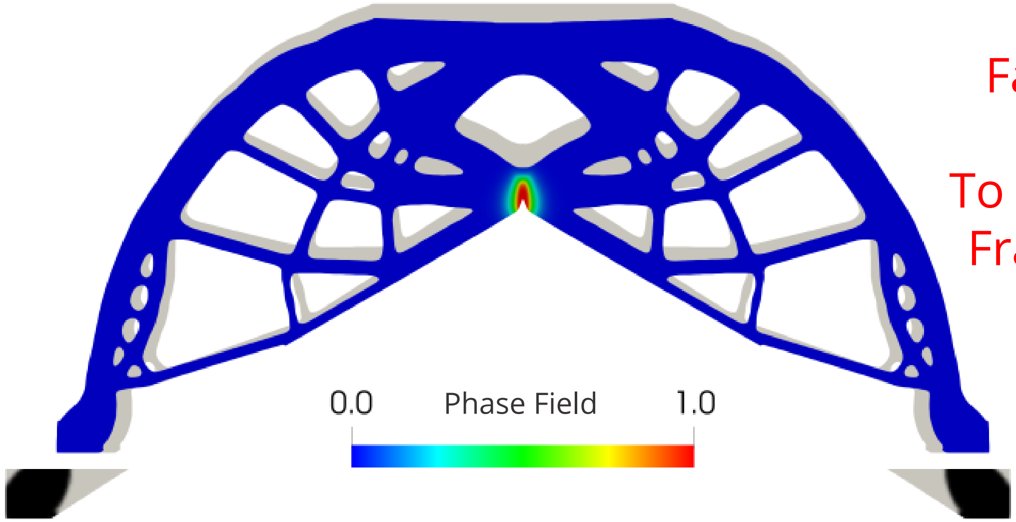

WB: Design with buckling only (omitting ductile failure)

WBF: Design with ductile failure constraints and buckling

Optimization problem reformulation

Minimize Volume Fraction Instead of Maximizing Work

$$
\begin{aligned}
\underset{\boldsymbol{\theta}}{\text{minimize}} \quad & \omega_1 \frac{VF(\boldsymbol{\theta})}{VF^{scale}} + \omega_2 \frac{B_{KS}(\boldsymbol{\theta}, \bar{\boldsymbol{u}}_L)}{B_{KS}^{scale}} + \omega_3 \; AL(\boldsymbol{\theta}, \{\bar{\boldsymbol{u}}_i\}, \{\boldsymbol{c}_i\}) \\
\text{subject to} \quad & 0 \leq \theta_e \leq 1, \; e = 1, \ldots, N_{elem} \\
& RF(\boldsymbol{\theta}, \{\bar{\boldsymbol{u}}_i\}, \{\boldsymbol{c}_i\}) \geq RF_{min} \\
& \boldsymbol{R}^{(i)}(\boldsymbol{\theta}, \{\bar{\boldsymbol{u}}_i\}, \{\boldsymbol{c}_i\}) = \boldsymbol{0}, \; i = 1, \ldots, N_{steps} \\
& \boldsymbol{H}^{(i)}(\boldsymbol{\theta}, \{\bar{\boldsymbol{u}}_i\}, \{\boldsymbol{c}_i\}) = \boldsymbol{0}, \; i = 1, \ldots, N_{steps} \\
& \boldsymbol{K}_L(\boldsymbol{\theta})\bar{\boldsymbol{u}}_L = \boldsymbol{f}_0 \\
& \boldsymbol{K}_\sigma(\boldsymbol{\theta}, \bar{\boldsymbol{u}}_L)\phi_i = \mu_i \boldsymbol{K}_L(\boldsymbol{\theta})\phi_i \text{ for } i \in \mathcal{B}
\end{aligned}
$$

Constrain Reaction Force Instead of Volume Fraction (→ applies to the constraint $RF(\boldsymbol{\theta}, \{\bar{\boldsymbol{u}}_i\}, \{\boldsymbol{c}_i\}) \geq RF_{min}$)

Portal frame numerical example

Without Failure & Buckling (VF 0.411)

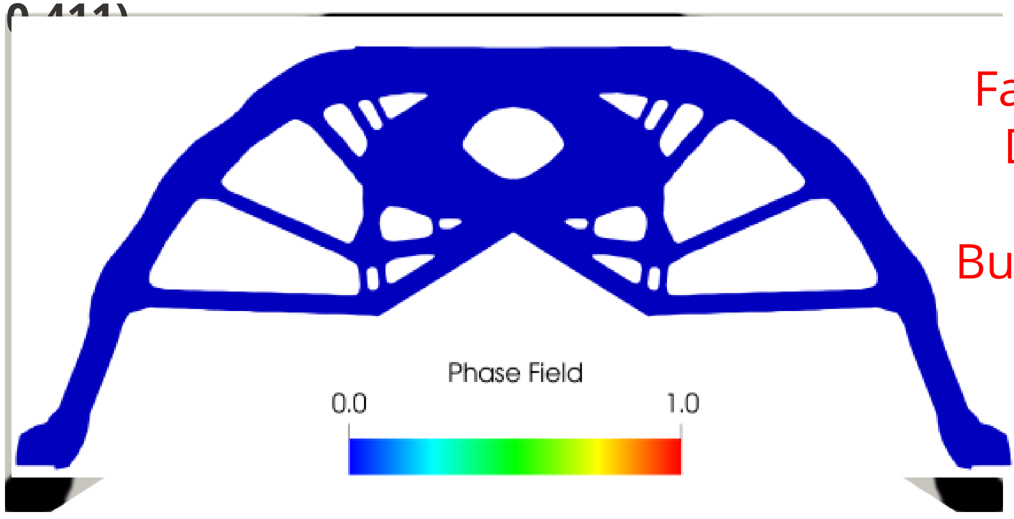

With Failure (VF 0.416)

+19.0% Peak Load
+428% Work
+8.5% Volume

Failure Due To Buckling

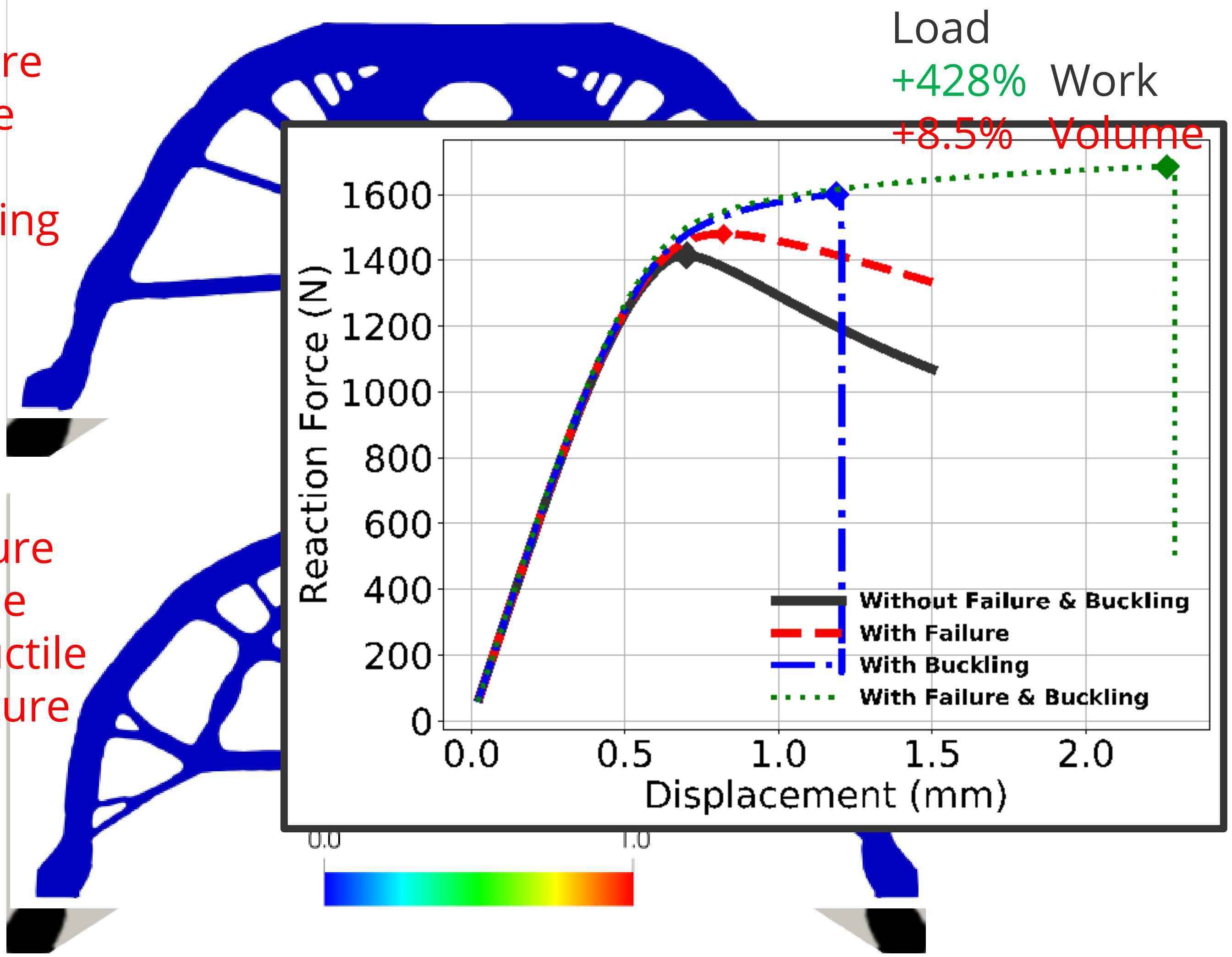

Failure Due To Ductile Fracture

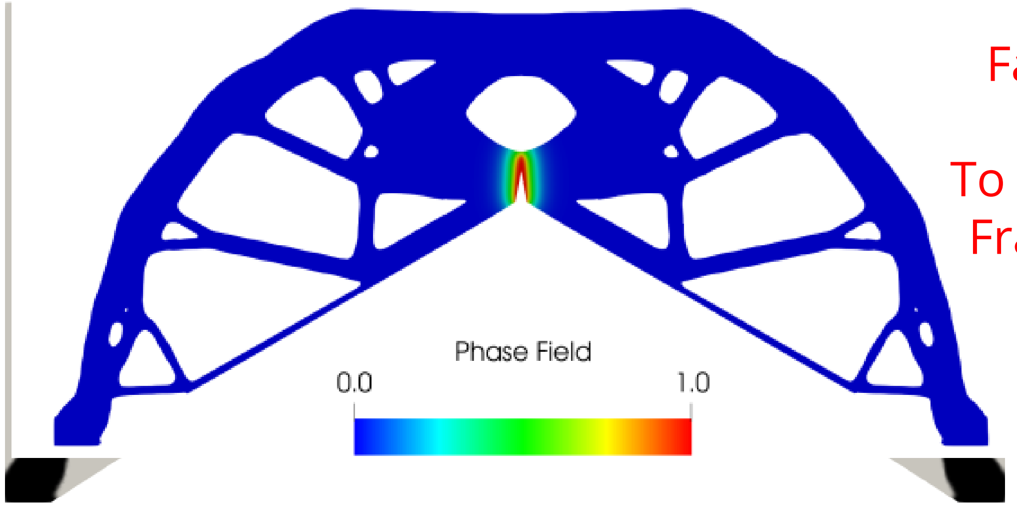

With Buckling (VF 0.427)

With Failure & Buckling (VF 0.446)

Concluding Remarks

- Demonstrated the importance of incorporating both failure constraints and buckling in design optimization
- Demonstrated, simple, computationally-efficient method for incorporating buckling resistance into topology optimization with ductile material physics
- Adapted Augmented-Lagrange local constraint methodology for elastoplastic local ductile failure indicators
- Demonstrated importance of verification step, either experimentally or with higher fidelity numerical models with large strain kinematics
- For more information please refer to the following publication:

Russ, J.B., Waisman, H., 2020b. A novel elastoplastic topology optimization formulation for enhanced failure resistance via local ductile failure constraints and linear buckling analysis. Computer Methods in Applied Mechanics and Engineering 373, 113478.

Back-up

Large strain ductile phase field fracture model

$$\boldsymbol{\tau}^{+}_{vol} = \begin{cases} J^e p \boldsymbol{I} & \text{if } \Theta \geq 1 \\ \boldsymbol{0} & \text{otherwise} \end{cases}$$

$$\boldsymbol{\tau}^{+}_{dev} = \mu \mathbb{P}_{dev} : \bar{\boldsymbol{b}}^e$$

$$\boldsymbol{\tau}^{-} = \begin{cases} \boldsymbol{0} & \text{if } \Theta \geq 1 \\ J^e p \boldsymbol{I} & \text{otherwise} \end{cases}$$

$$\boldsymbol{\tau} = \overline{g(c)}\boldsymbol{\tau}^{+}_{vol} + g(c)\boldsymbol{\tau}^{+}_{dev} + \boldsymbol{\tau}^{-}$$

$$\Theta = \frac{1}{V_0^e}\int_{\Omega_0^e} J \; dV_0$$

$$p = U'(\Theta) = \frac{\kappa}{2}\left(\Theta - \frac{1}{\Theta}\right)$$

$$\overline{g(c)} = \frac{1}{V_0^e}\int_{\Omega_0^e} g(c) \; dV_0$$

$$f\left(\boldsymbol{s}, \alpha\right) = ||\boldsymbol{s}|| - g_p(c)\sqrt{\frac{2}{3}}\sigma_y$$

$$\dot{W}_p = \dot{\gamma}\frac{||\boldsymbol{s}||}{\phi}$$

$$\phi(p, \boldsymbol{s}) = d_1 + d_2 \exp\left(d_3 \frac{p}{||\boldsymbol{s}||}\right)$$

$$\int_{\Omega_0^e} \boldsymbol{\tau}_n : \left(\nabla_0 \delta \boldsymbol{u} \cdot \boldsymbol{F}_n^{-1}\right) \; dV_0 = 0$$

$$\int_{\Omega_0^e} \left(\eta_v \frac{c_n - c_{n-1}}{\Delta t} + \frac{G_c}{2 l_0} c_n \; \delta c + 2 G_c l_0 \nabla_0 c_n \cdot \nabla_0 \delta c\right) \; dV_0 = \int_{\Omega_0^e} \left(g'(c_n) W^{+} + g_p'(c_n) \left\langle W_p - W_0 \right\rangle\right) \delta c \; dV_0$$

* Borden et al. 2016. A phase-field formulation for fracture in ductile materials, CMAME.

SIMP interpolation

Interpolation used for plasticity:

$$E = (\epsilon_e + (1 - \epsilon_e)\rho_e^p)\ E^{solid}$$
$$H = (\epsilon_p + (1 - \epsilon_p)\rho_e^q)\ H^{solid}$$
$$\sigma_{y_0} = (\epsilon_p + (1 - \epsilon_p)\rho_e^q)\ \sigma_{y_0}^{solid}$$
$$Y_\infty = (\epsilon_p + (1 - \epsilon_p)\rho_e^q)\ Y_\infty^{solid}$$

With hardening function:

$$\sigma_y(\alpha) = \sigma_{y_0} + H\alpha + Y_\infty\,(1 - \exp(-\delta\alpha))$$

Interpolation used for buckling:

$$E_L = (10^{-6} + (1 - 10^{-6})\rho_e^p)E^{solid}$$
$$E_\sigma = \rho_e^p E^{solid}$$

Sensitivity analysis

$$\frac{df}{d\boldsymbol{\rho}} = ?$$

$$\hat{f}(\boldsymbol{\rho}, \{\bar{\boldsymbol{u}}_i\}, \{\boldsymbol{c}_i\}) = f(\boldsymbol{\rho}, \{\bar{\boldsymbol{u}}_i\}, \{\boldsymbol{c}_i\}) + \sum_{n=1}^{N_{steps}} \boldsymbol{\lambda}_R^{n^T} \boldsymbol{R}_n(\boldsymbol{\rho}, \bar{\boldsymbol{u}}_n, \bar{\boldsymbol{u}}_{n-1}, \boldsymbol{c}_n, \boldsymbol{c}_{n-1}) + \sum_{n=1}^{N_{steps}} \boldsymbol{\lambda}_H^{n^T} \boldsymbol{H}_n(\boldsymbol{\rho}, \bar{\boldsymbol{u}}_n, \bar{\boldsymbol{u}}_{n-1}, \boldsymbol{c}_n, \boldsymbol{c}_{n-1})$$

Begin with last step

At step $n = N_{steps}$ one must solve

$$\frac{\partial \boldsymbol{R}_n}{\partial \bar{\boldsymbol{u}}_n}^T \boldsymbol{\lambda}_R^n + \frac{\partial \boldsymbol{H}_n}{\partial \bar{\boldsymbol{u}}_n}^T \boldsymbol{\lambda}_H^n = \underbrace{-\frac{\partial f}{\partial \bar{\boldsymbol{u}}_n}}_{\boldsymbol{F}_u}$$

$$\frac{\partial \boldsymbol{R}_n}{\partial \boldsymbol{c}_n}^T \boldsymbol{\lambda}_R^n + \frac{\partial \boldsymbol{H}_n}{\partial \boldsymbol{c}_n}^T \boldsymbol{\lambda}_H^n = \underbrace{-\frac{\partial f}{\partial \boldsymbol{c}_n}}_{\boldsymbol{F}_c}$$

for $\boldsymbol{\lambda}_R^n$ and $\boldsymbol{\lambda}_H^n$.

*i.e. the **last** step of the forward analysis*

Subsequently, traverse the forward analysis in backward order

At each step $n = \{N_{steps} - 1, N_{steps} - 2, \ldots, 3, 2, 1\}$ one must solve

$$\frac{\partial \boldsymbol{R}_n}{\partial \bar{\boldsymbol{u}}_n}^T \boldsymbol{\lambda}_R^n + \frac{\partial \boldsymbol{H}_n}{\partial \bar{\boldsymbol{u}}_n}^T \boldsymbol{\lambda}_H^n = \underbrace{-\frac{\partial f}{\partial \bar{\boldsymbol{u}}_n}^T - \frac{\partial \boldsymbol{R}_{n+1}}{\partial \bar{\boldsymbol{u}}_n}^T \boldsymbol{\lambda}_R^{n+1} - \frac{\partial \boldsymbol{H}_{n+1}}{\partial \bar{\boldsymbol{u}}_n}^T \boldsymbol{\lambda}_H^{n+1}}_{\boldsymbol{F}_u}$$

$$\frac{\partial \boldsymbol{R}_n}{\partial \boldsymbol{c}_n}^T \boldsymbol{\lambda}_R^n + \frac{\partial \boldsymbol{H}_n}{\partial \boldsymbol{c}_n}^T \boldsymbol{\lambda}_H^n = \underbrace{-\frac{\partial f}{\partial \boldsymbol{c}_n}^T - \frac{\partial \boldsymbol{R}_{n+1}}{\partial \boldsymbol{c}_n}^T \boldsymbol{\lambda}_R^{n+1} - \frac{\partial \boldsymbol{H}_{n+1}}{\partial \boldsymbol{c}_n}^T \boldsymbol{\lambda}_H^{n+1}}_{\boldsymbol{F}_c}$$

for $\boldsymbol{\lambda}_R^n$ and $\boldsymbol{\lambda}_H^n$.

Sensitivity analysis continued

If we label the right hand side of each equation in each of the aformentioned systems $\boldsymbol{F}_u$ and $\boldsymbol{F}_c$ and apply a Schur-complement technique, we arrive at the following system,

$$\left(\frac{\partial \boldsymbol{R}_n}{\partial \bar{\boldsymbol{u}}_n} - \frac{\partial \boldsymbol{R}_n}{\partial \boldsymbol{c}_n}\frac{\partial \boldsymbol{H}_n}{\partial \boldsymbol{c}_n}^{-1}\frac{\partial \boldsymbol{H}_n}{\partial \bar{\boldsymbol{u}}_n}\right)^T \boldsymbol{\lambda}_R^n = \boldsymbol{F_u} + \frac{\partial \boldsymbol{R}_n}{\partial \boldsymbol{c}_n}\frac{\partial \boldsymbol{H}_n}{\partial \boldsymbol{c}_n}^{-1}\boldsymbol{F_c}$$

$$\boldsymbol{\lambda}_H^n = \frac{\partial \boldsymbol{H}_n}{\partial \boldsymbol{c}_n}^{-1}\left(\boldsymbol{F_c} - \frac{\partial \boldsymbol{H}_n}{\partial \bar{\boldsymbol{u}}_n}\boldsymbol{\lambda}_R^n\right)$$

Assemble At Element Level

Fast Element Level Operations

which is mathematically beautiful and numerically efficient. Once the adjoint vectors are known, the computation of the sensitivities reduces to simple elemental operations.

$$\frac{df}{d\rho_e} = \frac{d\hat{f}}{d\rho_e} = \frac{\partial f}{\partial \rho_e} + \sum_{n=1}^{N_{steps}} \boldsymbol{\lambda}_R^{n\,T}\frac{\partial \boldsymbol{R}_n}{\partial \rho_e} + \sum_{n=1}^{N_{steps}} \boldsymbol{\lambda}_H^{n\,T}\frac{\partial \boldsymbol{H}_n}{\partial \rho_e}$$

Sensitivity analysis continued

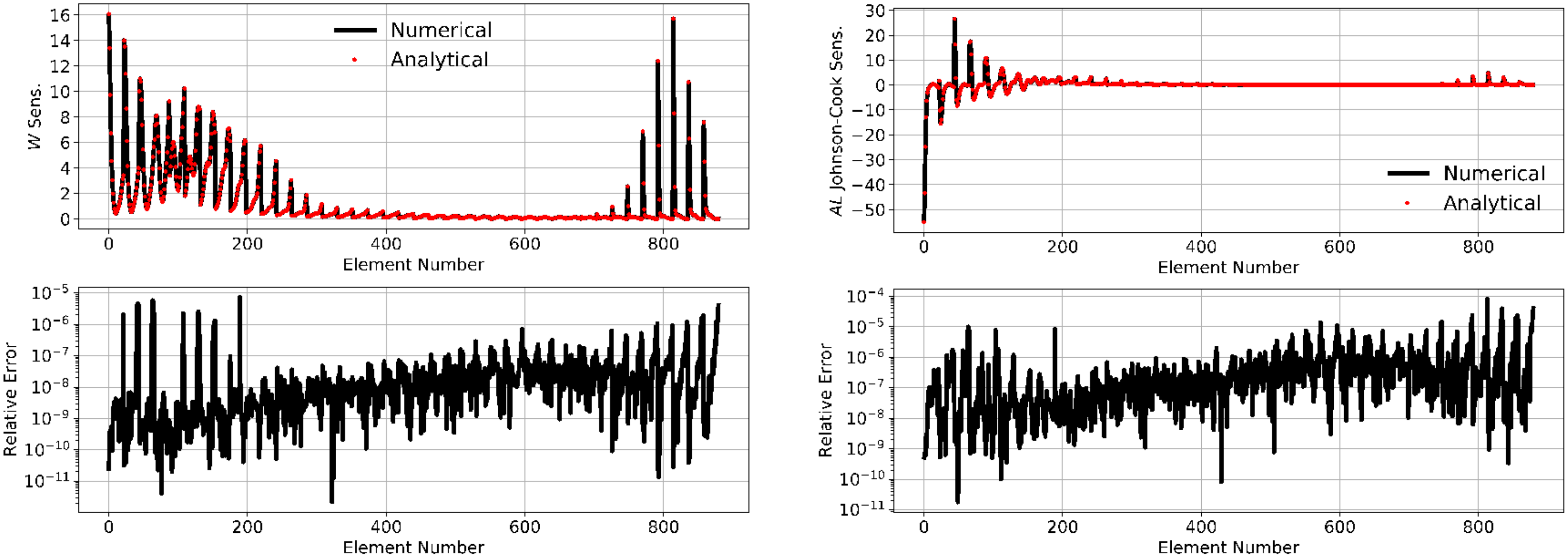

Numerical verification of sensitivities with finite differences

Topology Optimization for Ductile Failure and Buckling Resistance

W: Design only maximizing total work

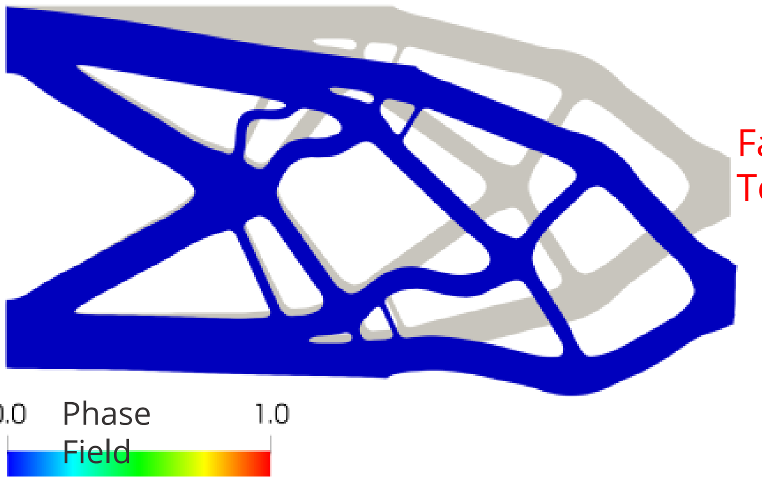

WF: Design for ductile failure (omitting buckling)

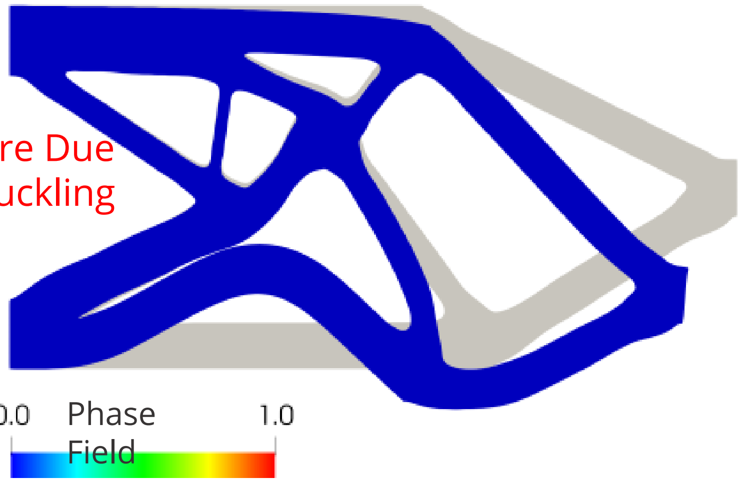

Failure Due To Buckling

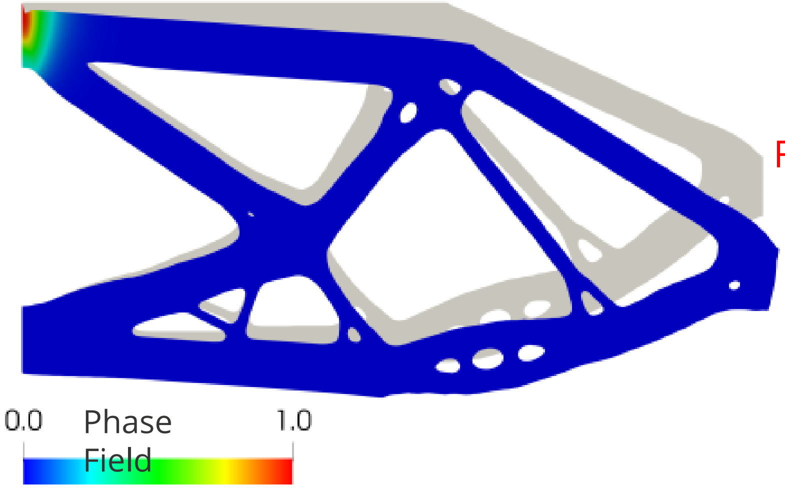

WB: Design for buckling only

Failure Due To Ductile Fracture

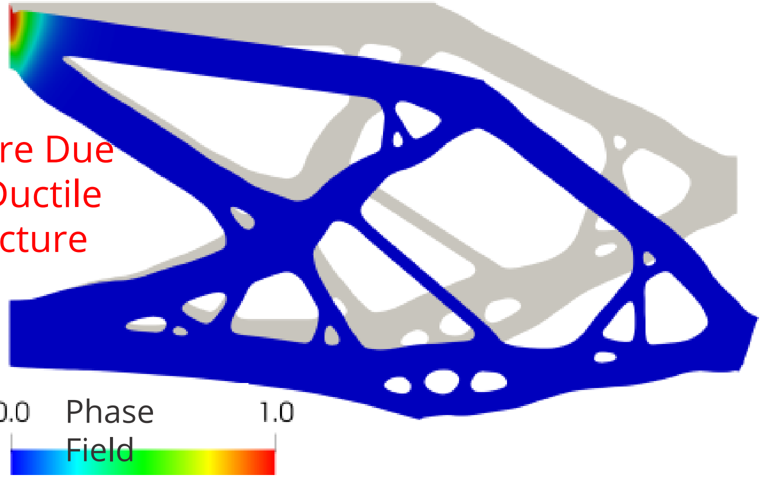

WBF: Design for ductile failure and buckling

+15.4% Peak Load
+899% Work To Peak Load Capacity

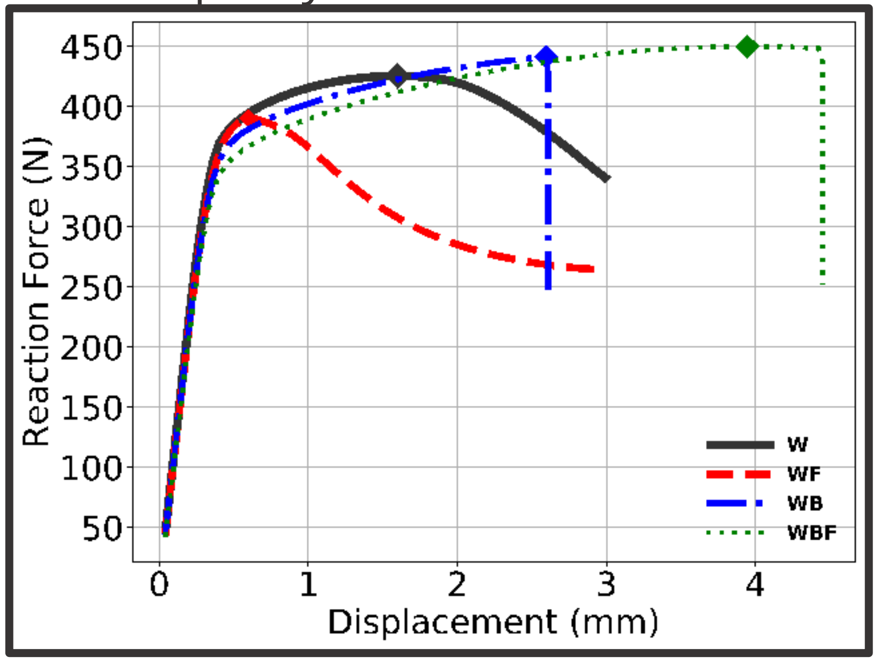

Calibrated constitutive model to test data provided for Aluminum 2024-T351